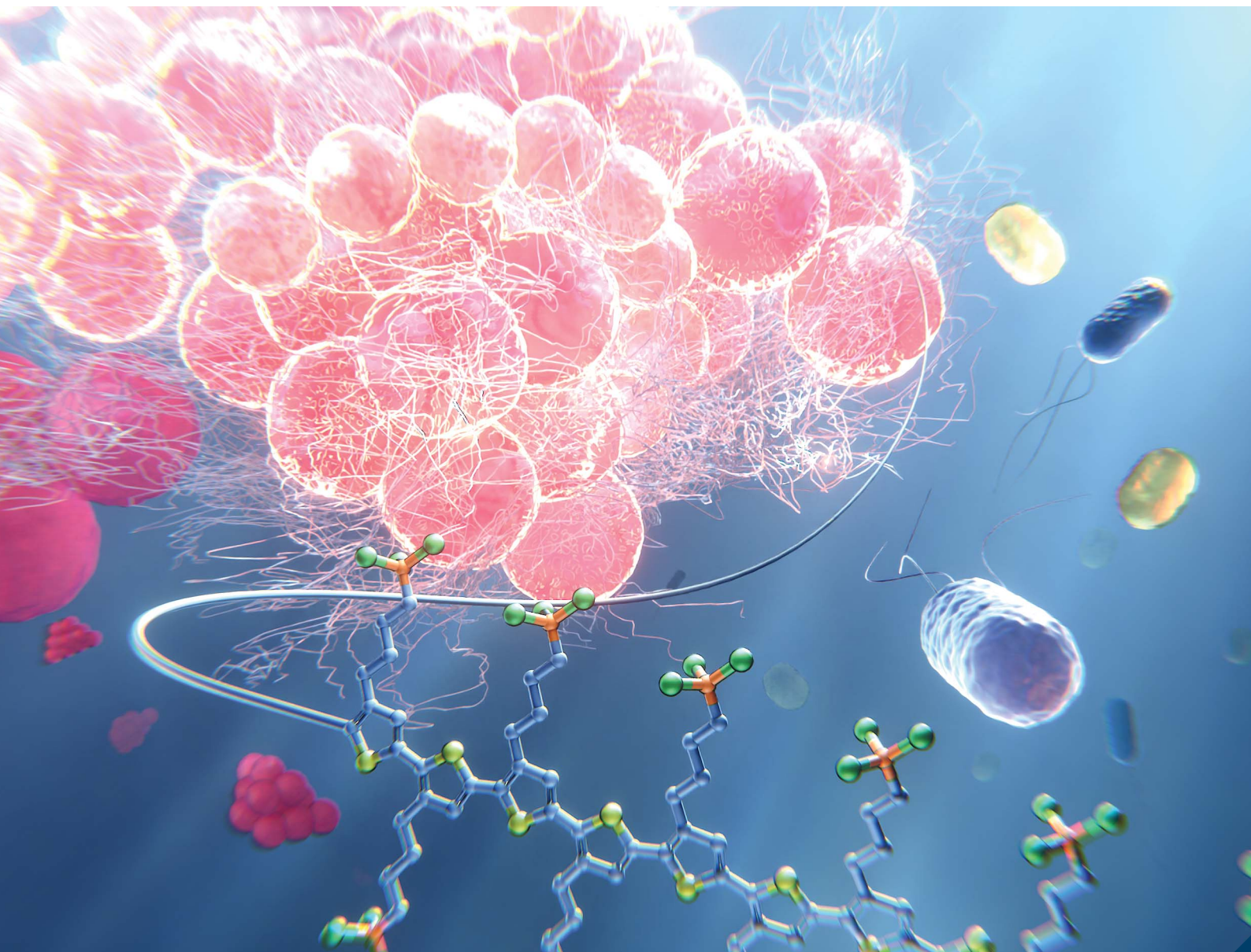


# Analytical Methods

rsc.li/methods



ISSN 1759-9679

**PAPER**

Yuko Takeoka *et al.*

Recognition and separation of Gram-positive and Gram-negative bacteria using polythiophene derivatives with phosphonium groups

Cite this: *Anal. Methods*, 2026, 18, 282Received 18th September 2025  
Accepted 28th November 2025

DOI: 10.1039/d5ay01570g

rsc.li/methods

## Recognition and separation of Gram-positive and Gram-negative bacteria using polythiophene derivatives with phosphonium groups

Hibiki Ogura,<sup>1</sup> Rui Kuroda, Nobuyuki Kanzawa, Takashi Hayashita,<sup>2</sup>  
Masahiro Yoshizawa-Fujita,<sup>1</sup> Masahiro Rikukawa<sup>1</sup> and Yuko Takeoka<sup>1</sup>

Water-soluble poly[3-(4-trimethylphosphinobutyl)thiophene bromide] (PTB), which has a phosphonium group at the end of its side chain and selectively recognizes and separates Gram-positive bacteria, was synthesized. Modifying its terminal group with an ethyl substitution greatly altered the bacterial response, notably causing abnormal fibrosis in Gram-negative *E. coli*.

Bacterial detection is of great importance from the perspective of disease diagnosis and public health. Although the effectiveness of antibiotics in treating bacterial infections is widely recognized, the increase in drug-resistant bacteria, due to their misuse and overuse, is a worldwide problem. Prophylactic antibiotic therapy is often implemented, but the use of antibiotics against a wide range of pathogens carries the risk of promoting the emergence of resistant strains.<sup>1,2</sup> Therefore, early identification of pathogens and targeted antimicrobial therapy are extremely important. The predominant bacterial detection methods currently in use, such as Gram staining, culture, turbidimetric, and PCR methods, have limitations such as long detection times and the requirement for special equipment.<sup>3–5</sup> Accordingly, the development of innovative sensing strategies capable of achieving rapid, facile, and precise bacterial identification has become increasingly imperative. Among the various candidates explored for biosensing applications,  $\pi$ -conjugated polymers, particularly polythiophene derivatives, have attracted considerable attention due to their intrinsic properties such as high electrical conductivity, optical responsiveness, and self-assembling behavior.<sup>6–10</sup> These characteristics can be finely modulated *via* molecular design, rendering them highly suitable for the development of advanced platforms.<sup>11–14</sup> Normally, polythiophene derivatives are insoluble in water. However, water-solubility can be achieved by modifying the side chain to a cationic group. A study by Ren *et al.* revealed that polythiophenes with quaternary ammonium groups exhibit

selective antibacterial activity against Gram-positive bacteria by inhibiting their growth.<sup>15</sup> It has been suggested that this property can be used to discriminate between Gram-positive and Gram-negative bacteria. Jiao *et al.* reported that quaternary ammonium compounds (QACs) have antimicrobial activity that acts on bacterial cell membranes and kill bacteria by causing membrane disruption and altered permeability.<sup>16</sup> However, it has been observed that long-term use of QACs can result in the development of bacterial resistance.<sup>16</sup> Therefore, if a method to discriminate between Gram-positive and Gram-negative bacteria without damaging the bacteria is established, it can be expected to reduce the risk of resistant bacteria and be applied as a new bacterial detection technology.

In this study, we aimed to detect and separate Gram-positive and Gram-negative bacteria using polythiophene with a phosphonium group, poly[3-(4-trimethyl phosphinobutyl)thiophene bromide] (PTB).  $\pi$ -Conjugated polymers can easily detect high molecular weight phosphoric compounds such as DNA and RNA and are expected to enable bacterial detection without bactericidal effects, due to their low cytotoxicity.<sup>17,18</sup> While Gram-positive bacteria have a thick cell wall with phosphate compounds, teichoic acid and lipoteichoic acid, on their surface,<sup>19</sup> Gram-negative bacteria have a thin cell wall covered by an outer membrane.<sup>20</sup> By using phosphonium polythiophenes, differences in phosphoric groups of the cell walls of Gram-positive and Gram-negative bacteria could be detected. We also investigated the effect of the phosphonium structure on the detection of bacteria and separate Gram-positive and -negative bacteria under co-culture conditions.

As a precursor polymer of PTB, poly(3-(4-bromobutyl)thiophene), PBBT, was synthesized from 2,5-dibromo-3-(4-bromobutyl)thiophene by the catalyst transfer condensation method (see the SI). The degree of polymerization (*n*) of PBBT was determined to be 11 by gel permeation chromatography. Water-soluble PTB was obtained after reacting PBBT with trimethylphosphite. As a series, poly[3-(4-triethylphosphinobutyl)thiophene bromide] (Et-PTB) and poly[3-(4-tri-phenylphosphinobutyl)thiophene bromide] (Ph-PTB) were

Department of Materials and Life Sciences, Sophia University, 7-1 Kioi-cho, Chiyoda-ku, Tokyo 102-8554, Japan. E-mail: y-tabuch@sophia.ac.jp



obtained from **PBBT** with the same  $n$  value ( $n = 11$ ). The phosphonium conversion ratios of **PTB**, **Et-PTB**, and **Ph-PTB** were in the range of 95–99%, as determined by  $^1\text{H}$  NMR. Gram-positive, *Staphylococcus aureus* and *Bacillus subtilis*, and Gram-negative bacteria, *Escherichia coli* and *Pseudomonas aeruginosa*, were used. Luria broth (LB) medium and a suspension of each bacterium were added to individual tubes and adjusted to a final concentration of  $1.0 \times 10^4$  cells  $\text{mL}^{-1}$ . The cultures were shaken ( $37^\circ\text{C}$ , 180 rpm) following the addition of a Tris-HCl buffer solution containing individual phosphonium polymers ( $1.0 \text{ g L}^{-1}$ ). The optical density at 600 nm ( $\text{OD}_{600}$ ) was measured as a function of time using a UV-Visible spectrophotometer.

Fig. 1 shows the growth curves of (a) *S. aureus*, (b) *B. subtilis*, (c) *E. coli*, and (d) *P. aeruginosa* versus incubation time. All bacterial concentrations at the start of the culture were equalized to  $1.0 \times 10^4$  cells  $\text{mL}^{-1}$ . In the absence of **PTB**,  $\text{OD}_{600}$  values for all bacteria began to increase after 5 h of culture and exceeded 1.5 after 24 h. In the presence of **PTB**, the growth curve characteristics varied depending on the type of bacteria. With **PTB** for (a) *S. aureus* and (b) *B. subtilis*, the  $\text{OD}_{600}$  values remained at 0.0 over 24 h. In contrast, the growth curves of (c) *E. coli* and (d) *P. aeruginosa* were indistinguishable in the absence and presence of **PTB**, indicating that **PTB** did not affect their growth. It can be deduced that the outer membrane of Gram-negative bacteria prevented **PTB** uptake and penetration, and thus **PTB** had no effect on the bacteria.<sup>21,22</sup> These observations indicate that **PTB** recognizes differences in bacterial surface structures and exhibits antibacterial activity only against Gram-positive bacteria. This phenomenon results from interactions between anionic compounds on the bacterial surface and cationic side chains, causing changes in surface charge.<sup>15</sup> Because Gram-positive bacteria show a greater shift in zeta potential than Gram-negative bacteria, surface charge appears to influence bacterial adsorption. Because teichoic and lipoteichoic acids are abundant and directly exposed on the

surface of Gram-positive bacteria, whereas these anionic groups are shielded by an outer membrane in Gram-negative bacteria, surface charge density is most likely the primary determinant of selective recognition. The antibacterial properties of **PTB** were assessed using the disk diffusion method. This assay revealed no zone of inhibition for any of the tested Gram-positive or Gram-negative bacteria, thus demonstrating the non-bactericidal nature of **PTB**. We have done similar experiments on a **PBBT** derivative bearing an ammonium end group, and no clear difference was observed between Gram-positive and Gram-negative bacteria, indicating that antimicrobial activity is dependent on the cation species (Fig. S10).

To investigate the relationship between bacterial concentration and **PTB**, cultures with different initial bacterial concentrations were conducted. Fig. 2(a) shows the growth curves of *S. aureus* ( $1.0 \times 10^4$ ,  $1.0 \times 10^6$ , and  $1.0 \times 10^8$  cells  $\text{mL}^{-1}$ ) in the presence of  $1.0 \text{ g L}^{-1}$  **PTB**. The concentration of *S. aureus* without **PTB** was  $1.0 \times 10^4$  cells  $\text{mL}^{-1}$ . While S4/**PTB** ( $1.0 \times 10^4$  cells  $\text{mL}^{-1}$  of *S. aureus* with **PTB**) showed no increase in turbidity during the 24 h incubation, the  $\text{OD}_{600}$  value of S6/**PTB** and S8/**PTB** increased and the values at 24 h were dependent on the initial concentration of the bacterial suspension. This indicates that **PTB** did not fully suppress growth under the S6 and S8 conditions, and the molar amount ( $3.3 \times 10^6 \text{ mol g}^{-1}$ ) of phosphonium groups of **PTB** used was not sufficient to completely suppress *S. aureus* growth at concentrations greater than  $1.0 \times 10^6$  cells  $\text{mL}^{-1}$ . To investigate the reason for the concentration dependence on turbidity, fluorescence measurements and fluorescence microscope observation were performed after 24 h of incubation. Fig. 2(b) shows the fluorescence spectra of S4/**PTB**, S6/**PTB**, and S8/**PTB** samples after 24 h of incubation. Here, the excitation wavelength was set to 410 nm, which is the maximum absorption wavelength of **PTB**. S4/**PTB** showed higher fluorescence around 500 nm, which originated from free **PTB** that remained in the solution. The fluorescence intensity decreased and the peak shifted to a longer wavelength as the initial bacterial concentration increased. Differences in fluorescence were observed, suggesting alterations in the state of **PTB** and indicating that less **PTB** was dissolved in the S6/**PTB** and S8/**PTB** solutions. The critical suspension concentration at which *S. aureus* growth could be inhibited using **PTB** under these experimental conditions was

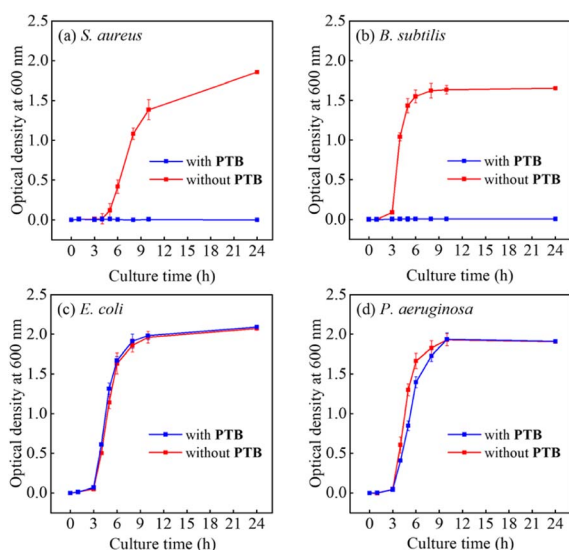


Fig. 1 Growth curves of (a) *S. aureus*, (b) *B. subtilis*, (c) *E. coli*, and (d) *P. aeruginosa* in the absence and presence of **PTB**.

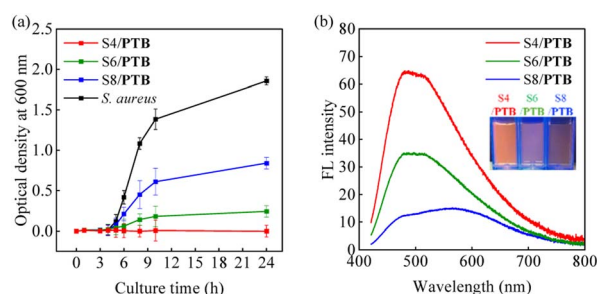


Fig. 2 (a) Growth curves and (b) fluorescence ( $\lambda_{\text{ex}} = 410 \text{ nm}$ ) spectra of *S. aureus*/**PTB**. Inset shows a photo of S4, S6, and S8/**PTB** solutions under UV light irradiation.  $S_m$  indicates that the concentration of *S. aureus* is  $1.0 \times 10^m$  cells  $\text{mL}^{-1}$ .



found to be between  $1.0 \times 10^4$  and  $1.0 \times 10^6$  cells  $\text{mL}^{-1}$ .<sup>23</sup> More growth was observed at higher bacterial concentrations, suggesting that **PTB** lacks overt bactericidal activity. Instead, it appears that **PTB** inhibits the growth of bacteria, indicating that it functions more as a bacteriostatic agent.

Fig. 3 shows fluorescence microscope images and illustrations of (a) *S. aureus*, (b) S4/**PTB**, and (c) S8/**PTB** after 24 h of incubation. As shown in Fig. 3(a), in the absence of **PTB**, *S. aureus* was dispersed. In contrast, the S4/**PTB** condition exhibited large fluorescent aggregates (red regions) of around several tens of microns. Under the S8/**PTB** condition, dispersed bacteria were observed, with each particle showing **PTB** fluorescence (red regions). These phenomena can be explained by the illustration in Fig. 3. When there are more **PTB** molecules per bacterium, **PTB** behaves as a glue to connect *S. aureus* to form large aggregates. By increasing the initial concentration of *S. aureus*, the number of **PTB** molecules per *S. aureus* decreases and bacterial dispersion with low **PTB** was observed as fluorescence particles. The results of the zeta potential support this estimation. The zeta potential is  $-28$  mV for **PTB**, suggesting that the negative charges of the phosphate groups repel each other and are dispersed. The zeta potential was  $-27$  mV for S8/**PTB**. In this system, since there are fewer **PTB** molecules per bacterium, the very small amount of negative charge is compensated for by the interaction of **PTB** and *S. aureus*, and the bacteria are thought to be dispersed by repulsion of negative charges. On the other hand, the zeta potential of S4/**PTB** is  $-7$  mV, which is smaller than that of *S. aureus* alone and S8/**PTB**. This means that the negative charges of the bacterium are canceled, and the bacteria are thought to attract each other, forming large aggregates. In the case of S4/**PTB**, **PTB** exerts its antimicrobial action by aggregating a small number of bacteria. In the S4/**PTB** system, **PTB** may inhibit the survival and growth of bacteria by causing them to strongly attract each other and form large aggregates. Therefore, the antimicrobial mechanism of **PTB** is thought to involve not only changes in the surface charge of bacteria but also aggregation of bacteria and inhibition of bacterial growth under certain conditions.

By utilizing the specific aggregation properties of **PTB** against Gram-positive bacteria, we attempted to separate Gram-

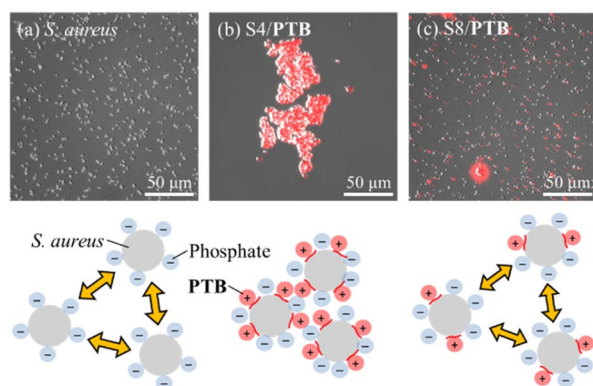


Fig. 3 Fluorescence microscope images and illustration of (a) *S. aureus*, (b) S4/**PTB** and (c) S8/**PTB** after 24 h of incubation.

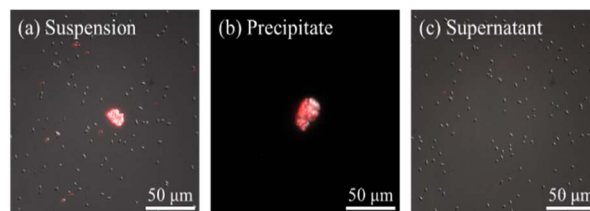


Fig. 4 Fluorescence microscope images of (a) the suspension containing *S. aureus* and *E. coli*, (b) the precipitate, and (c) the supernatant after centrifugation of (a).

positive bacteria from a mixture of Gram-positive and Gram-negative bacteria. After 10 h of cultivation, the mixture containing *S. aureus* and *E. coli* was subjected to centrifugation. Fig. 4 shows fluorescence microscopy images of (a) the suspension before centrifugation, (b) the precipitate, and (c) the supernatant after centrifugation. In Fig. 4(a), aggregated bacteria were observed among many dispersed bacteria. The aggregates emitted fluorescence, indicating that the presence of **PTB**. *S. aureus* was aggregated by **PTB**, and its growth was inhibited. On the other hand, *E. coli* grew without the formation of aggregates. In Fig. 4(b), aggregated bacteria were observed, suggesting that they were *S. aureus* aggregated by **PTB**. In Fig. 4(c), only dispersed bacteria were observed, suggesting the presence of *E. coli*. Thus, it was possible to separate the mixed *S. aureus* and *E. coli* by using **PTB**. **PTB** acts specifically on *S. aureus*, changing its surface charge and causing bacterial aggregation. On the other hand, **PTB** has little effect on *E. coli*, which remains dispersed, allowing effective separation of the two bacteria by centrifugation. Such selective agglutination of **PTB** may be useful in the development of bacterial identification and separation techniques.

To investigate the effect of the phosphonium structure of polythiophenes on bacterial recognition,  $1.0 \times 10^4$  cells  $\text{mL}^{-1}$  of *S. aureus* were incubated with **Et-PTB** and **Ph-PTB**, which are similar to **PTB**. Fig. 5 shows  $\text{OD}_{600}$  after 24 h of culture of *S. aureus* with added **PTB**, **Et-PTB**, and **Ph-PTB**. For *S. aureus* alone,  $\text{OD}_{600}$  reached almost 2.0. Meanwhile, in the other samples, the  $\text{OD}_{600}$  differed depending on the phosphonium polythiophenes added. An  $\text{OD}_{600}$  of about 0.0 was observed for **PTB** and **Et-PTB**, and about 0.3 for **Ph-PTB**. The results suggest that the strength of antimicrobial activity against *S. aureus* varies depending on

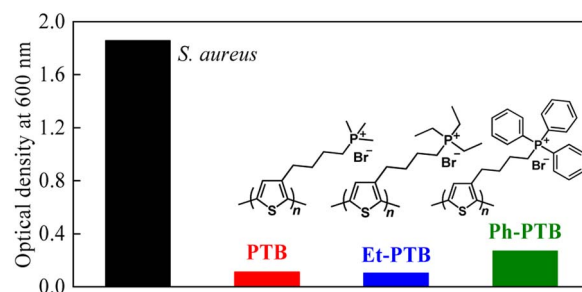


Fig. 5  $\text{OD}_{600}$  after 24 h of incubation of *S. aureus* with added **PTB**, **Et-PTB**, or **Ph-PTB**.



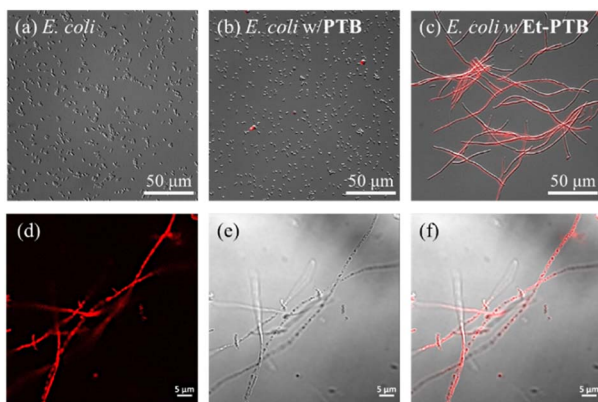


Fig. 6 Fluorescence microscope images of (a) *E. coli*, (b) *E. coli* w/PTB and (c) *E. coli* w/Et-PTB after 24 h of incubation. (d) Enlarged fluorescence microscope image and (e) clairvoyance image of (c). (f) Overlaid image of (d) and (e).

the structure of the phosphonium group. In the comparison of PTB, Et-PTB, and Ph-PTB, it was observed that the less bulky the electrostatic interaction with the bacteria, the greater the antimicrobial activity exhibited. This suggests that the size of the substituents around the phosphonium groups is an important factor that affects the antimicrobial effect against *S. aureus*.

As mentioned above, PTB showed no effect on the growth on *E. coli*; however, Et-PTB had a notable effect on *E. coli* morphology. Fig. 6 shows the fluorescence microscopy images of (a) *E. coli*, (b) *E. coli* w/PTB, and (c) *E. coli* w/Et-PTB after 24 h of incubation (the initial concentration of bacteria was  $1.0 \times 10^4$  cells mL<sup>-1</sup>). In (a) and (b), *E. coli* was observed to grow and disperse normally. On the other hand, in (c), fibrosis was induced in *E. coli* by the addition of Et-PTB. Fibrosis of *E. coli* is caused by inhibition of DNA replication and peptidoglycan synthesis due to stress factors such as the presence of antibiotics, environmental changes, nutrient deficiency, etc.<sup>24,25</sup> Since PTB contains trimethyl phosphonium groups and Et-PTB has triethyl phosphonium groups, the hydrophilic/hydrophobic balance on the bacterial surface in the presence of Et-PTB is altered; thus, the action of PTB or Et-PTB on *E. coli* differs. The hydrophobicity of Et-PTB may have been a stress factor for *E. coli*. In (d)–(f), we can observe fluorescent Et-PTB along the fibrous *E. coli*. This indicates that a micron scale interaction between Et-PTB and the surface anionic part of *E. coli* induces a macroscopic morphological change. Existing materials often either lack selectivity by acting on both Gram-positive and Gram-negative bacteria, or they require the conjugation of an antibiotic to achieve selectivity, which introduces the risk of antimicrobial resistance.<sup>26,27</sup> In contrast, our results proved the advantages of PTB against selectivity, a non-destructive mechanism, and dual functionality for detection and separation.

In summary, the polythiophene with a phosphonium group showed inhibition of Gram-positive bacteria but had no effect on Gram-negative bacteria. It is possible to discriminate between bacteria without killing them. In a mixed culture, PTB selectively agglutinated *S. aureus*, allowing its separation from *E. coli* by centrifugation. The interaction between the polymers

and bacteria was dependent on the phosphonium structure. Notably, Et-PTB induced fibrosis of *E. coli*, potentially having utility in the production of biofilms. Further investigation of the mechanism of Et-PTB is now underway.

## Conflicts of interest

There are no conflicts to declare.

## Data availability

The supporting data has been provided as part of the Supplementary information (SI). Supplementary information: synthetic procedures of monomers and polymers, elemental analysis of compounds, and other experimental data. See DOI: <https://doi.org/10.1039/d5ay01570g>.

## Notes and references

- 1 P. Askari, M. H. Namaei, K. Ghazvini and M. Hosseini, *BMC Pharmacol. Toxicol.*, 2021, **22**, 42.
- 2 S. Zhu, X. Wang, Y. Yang, H. Bai, Q. Cui, H. Sun, L. Li and S. Wang, *Chem. Mater.*, 2018, **30**, 3244.
- 3 S. R. Vartoukian, R. M. Palmer and W. G. Wade, *FEMS Microbiol. Lett.*, 2010, **309**, 1.
- 4 A. Mikagi, Y. Takahashi, N. Kanzawa, Y. Suzuki, Y. Tsuchido, T. Hashimoto and T. Hayashita, *Molecules*, 2023, **28**, 4.
- 5 H.-J. Kim, H.-J. Lee, K.-H. Lee and J.-C. Cho, *Food Control*, 2012, **23**, 491.
- 6 Q. Li, Y. Li, L. Ding, X. Li, J. Ma, T. Minami and S. Sang, *Microchemical J.*, 2025, **215**, 114484.
- 7 I. Abdel Aziz, G. Tullii, M. R. Antognazza and M. Criado-Gonzalez, *Mater. Horiz.*, 2025, **12**, 5570.
- 8 S. M. Tawfik, M. Sharipov, M. R. Elmasry, S. Azizov, D.-H. Kim, A. Turaev, Y.-I. Lee and H. Eui Jeong, *Microchemical J.*, 2024, **207**, 111947.
- 9 A. K. Nandi, *Langmuir*, 2024, **40**, 9385.
- 10 B. Mohan, Y. Sasaki and T. Minami, *Smart Molecules*, 2024, **2**, e20240001.
- 11 K. Sugiyasu, C. Song and T. M. Swager, *Macromolecules*, 2006, **39**, 5598.
- 12 M. Leclerc and K. Faid, *Adv. Mater.*, 1997, **9**, 1087.
- 13 T. Hirahara, M. Yoshizawa-Fujita, Y. Takeoka and M. Rikukawa, *Chirality*, 2018, **30**, 699.
- 14 Y. Takeoka, F. Saito and M. Rikukawa, *Langmuir*, 2013, **29**, 8718.
- 15 X. Ren, J. Hao, L. L. Guo, G. Sathishkumar and L. Q. Xu, *Polym. Bull.*, 2022, **79**, 2747.
- 16 Y. Jiao, L. N. Niu, S. Ma, J. Li, F. R. Tay and J. H. Chen, *Prog. Polym. Sci.*, 2017, **71**, 53.
- 17 Y. Xue, H. Xiao and Y. Zhang, *Int. J. Mol. Sci.*, 2015, **16**, 3626.
- 18 S. Hladys, A. Murmiliuk, J. Vohlidal, D. Havlicek, V. Sedlarik, M. Stepánek and J. Zedník, *Eur. Polym. J.*, 2018, **100**, 200.
- 19 W. W. Navarre and O. Schneewind, *Microbiol. Mol. Biol. Rev.*, 1999, **63**, 174.
- 20 T. J. Beveridge, *J. Bacteriol.*, 1999, **181**, 4725.



- 21 M. C. Jennings, K. P. Minbiole and W. M. Wuest, *ACS Infect. Dis.*, 2015, **1**, 288.
- 22 D. Kwasniewska, Y. L. Chen and D. Wiczorek, *Pathogens*, 2020, **9**, 493.
- 23 Y. Huang, H. C. Pappas, L. Q. Zhang, S. S. Wang, R. Ca, W. H. Tan, S. Wang, D. G. Whitten and K. S. Schanze, *Chem. Mater.*, 2017, **29**, 6389.
- 24 D. C. Karasz, A. I. Weaver, D. H. Buckley and R. C. Wilhelm, *Environ. Microbiol.*, 2022, **24**, 1.
- 25 S. S. Yadavalli, J. N. Carey, R. S. Leibman, A. I. Chen, A. M. Stern, M. Roggiani, A. M. Lippa and M. Goulian, *Nat. Commun.*, 2016, **7**, 12340.
- 26 M. Guo, K. Zhou, R. Ding, X. Zhao, Y. Zhang, Z. Zhang and G. He, *J. Mater. Chem. B*, 2022, **10**, 3097.
- 27 L. Gui Ning, S. Wang, X. Feng Hu, C. Ming Li and L. Qun Xu, *J. Mater. Chem. B*, 2017, **5**, 8814.

